Lasing emission from ZnO hierarchical micro-spherical microcavity

Ryosuke Komatsu,[1] Sota Yoshino, [1] Noriko Saito,[2] and Taisei Yamamoto,[3] Toshihiro Nakamura,[1]*

[1] Department of Electronic and Electronics, Hosei University, Koganei, Tokyo 184-8584, Japan

[2] National Institute for Materials Science, 1-1 Namiki, Tsukuba 3050044, Japan

[3] SANKEN (The Institute of Scientific and Industrial Research), Osaka University, 8–1 Mihogaoka, Ibaraki, Osaka 567–0047, Japan.

KEYWORDS: random laser, ZnO, micro laser, nanotechnology, light scattering efficiency, excited carriers

ABSTRACT:

We investigated lasing characteristics of a ZnO hierarchical micro-spherical particles with diameters of 1 – 5 μm. The lasing emission consists of a small number of discrete laser peaks unlike conventional random lasing from ZnO nanopowder-assembly. Theoretical calculations based on a many-body theory revealed that the optical gain is achieved at the observed lowest lasing threshold value, $4\ \mathrm{mJ \cdot cm^{-2} \cdot pulse^{-1}}$, which corresponds to the excited carrier density $\sim 2.4 \times 10^{25}\ \mathrm{m^{-3}}$. Because the carrier density is much higher than the Mott density, the gain origin for lasing is electron-hole plasma recombination. The lasing frequency mode shift (~ 1.2 meV) is due to the refractive index change induced by exciting high carrier density up to $6.1 \times 10^{25}\ \mathrm{m^{-3}}$.

By changing hierarchical structures via controlling growth condition and performing the annealing treatment and performing the calculation of scattering efficiency of ZnO particles, we found that the hierarchy of the micro-spherical particle plays a crucial role of the lasing feedback: the strong light scattering at the interface between outer nanoparticles with the sizes of 100 – 200 nm and smaller ones with the sizes of 10 – 60 nm consisting in the micro-spherical particle results in a light confinement. Furthermore, it has been confirmed that each discrete lasing mode shows strong gain competition with each other probably due to spatial overlap between the modes. These results suggest that both random scattering and microcavity modes contribute to the lasing oscillation.

1. Introduction

It is well known that for lasing operation the design of the laser cavity is essential. For example, a usual semiconductor laser diode consists of a direct gap semiconductor acting as an optical gain active layer and sandwiched between n-type and p-type carrier conducting semiconductor layers.[1–3] An optical confinement occurs due to the waveguide effect caused by the difference in the refractive index between the active layer and sandwiching layers, resulting in the amplification of light emitted from active layer due to positive feedback with particular cavity modes.[4] Thus, the precise control of the cavity structure is a key issue for the laser operation. In other words, lasing characteristics such as lasing thresholds and modes (e.g., frequency modes and spatial modes) of a laser device are determined by cavity structure properties. Random laser is an interesting counterpart of conventional lasers because of their distinguish differences in its cavity structure shape from the lasers, i.e., it simply consists only of an optical gain medium and light scatterers which randomly positioned inside or outside the gain medium.[5] Pumping the gain

medium causes non-uniform multiple scattering of the emitted light by the scatterers, various cavity modes randomly form and subsequently, optical amplification occurs.[6] Because of intrinsic randomness of cavity modes, the frequency modes of the random laser are continuous over a wide wavelength range,[7] and thus, random lasing emission usually appears at the peak position of the gain spectrum.[8] Because random lasers do not require a precise control of cavity structure, they can be easily fabricated, and they are expected to be applied to a low-cost and high-power laser incoherent illumination source.[9]

Various configurations of random lasers have been reported, such as dye-based random lasers [5,10–17] which consists of organic molecules as an optical gain medium and dielectric and semiconductor nanostructures as light scatterers. Titanium dioxide or aluminum oxide which have a relatively high refractive index are often used as a scatterer material. There is also another type of random laser called a powder laser, where fine particles typically obtained by grinding laser glass such as neodymium doped yttrium aluminum garnet which is commonly used in ordinary solid-state lasers serve as both optical gain medium and scatterers.[18–20] This type of the lasers has significant advantages such as simplicity of the component (i.e., only powder assembly) and high durability to environmental changes and degradation due to high pumping.

One type of powder laser is a semiconductor random laser composed of direct-gap semiconductors such as zinc oxide (ZnO) [21], gallium arsenide [22], gallium nitride [23,24], and semiconductor quantum dots [25–33]. Semiconductor random lasers have significant advantages for applications, such as the possibility of electrical excitation [34–36]. Various shapes of semiconductor nanostructures as a random laser component have been used: the most common ones are nanoparticles [37–39] and nanowires (nanorods) [40–44] with the diameters of a few hundred nanometers. In this system, multiple light-scattering between nanostructures and subsequent optical amplification are contributed to lasing oscillation. Due to their randomness,

strongly fluctuated frequency multi-mode structures appear on the emission spectrum, and it is difficult to control the number of lasing peaks and the intensity[45]. Furthermore, large background spontaneous light emission band was observed because of inevitable scattering loss.

There is a different type of semiconductor random lasers where a single micro-particle such as an aggregate of ZnO nanoparticles[46,47] and an irregular shaped sintered ZnO micro-particle[48–50] is only the component. In contrast to conventional random lasers, quasi-single mode lasing spectrum has been overserved with quite low background spontaneous emission. Such lasing properties as well as easiness of lasing structure fabrication are promising for realizing micro-random laser devices under a low number of frequency mode operation. Such a high-quality and low mode lasing emission is attributed to optical confinement in scattered lights inside a micro-particle. In the case of the irregular shaped micro-particle, light scattering events are considered to only occur at the interface between the particle and outside medium (air). For the micro-aggregate, because all the nanoparticles consisting in the aggregate scatter emitted lights, the scattering events contributing to optical feedback could exist at the whole part of the micro-aggregate. Thus, the essential component of the aggregate for the optical confinement inducing the mode-controlled lasing is unclear. In this study, we focus on a ZnO micro-spherical particle aggregate consisting of nanoparticles with hierarchical size variation from several tenth to hundreds of nanometers in diameters. We prepare the micro-spherical particles by our originally developed solvothermal process[51–53] and investigate the detailed lasing characteristics of them. By changing the hierarchical components to clarify essential scattering centers for optical feedback to lase, we find that the strong light scattering by outer nanoparticles with the sizes of 100 – 200 nm covering on inner smaller particles results in light confinement and resultant formation of random cavity modes inside the micro-spherical particle.

2. Experimental

We prepared spherical ZnO hierarchical micro-spherical particles by a solvothermal growth method in ethylene glycol (EG) and water solution added hexamethylenetetramine (HMT). In brief, the preparation process is as follows: Zinc acetate anhydride used as a precursor of ZnO particles and HMT were dissolved in EG/water solution. The solution was moderately heated at temperatures at around ~100^{o}C. Spherical ZnO micro-spherical particles form due to the promotion of hydrolysis reactions of zinc acetate and HMT. The variation of the temperatures and treatment time allows us to easily control the hierarchical structure. In present work, we prepared two samples with the thermal reaction treatments at 95^{o}C and 120^{o}C for 12 h, which clearly different morphologies described below. The size range of the prepared micro-spherical particles were ~1 – 5 μm. Then, as-prepared ZnO micro-spherical particle samples were annealed at 400°C for 2 hours in an ambient atmosphere to further vary the morphology and crystallinity of the samples. We confirmed that the crystallite sizes are almost the same value (~30 nm) between the as-prepared and annealed micro-spherical particles by using the x-ray diffraction measurements.

For optical measurements, the prepared ZnO micro-spherical particles were dispersed in ethanol and then the solution was spin-coated on a silicon substrate. By adequately controlling the concentration of ZnO micro-spherical particles and coating condition, we obtained well mono-dispersedly deposited ZnO particle samples. For a reference purpose, a conventional ZnO nanopowder assembly random laser[38] was prepared by depositing ZnO nanoparticles (Alfa Aesar) with the average diameter of ~200 nm on the substrate. For these samples, photoluminescence (PL) and lasing measurements were performed. In PL measurements, continuous wave (CW) light at 325 nm from He-Cd laser (KIMMON KOHA, IK3452R-F) was used as an optical excitation. In lasing measurments, pulsed pumping laser light source (Teemphotonics, STV-01E) with the wavelength of 355 nm, a pulse duration of 200 ps and a

repetition rate of 2 kHz was employed. The photo-emission from the samples were detected from a multichannel charge coupled device (CCD) equipped spectrograph (Roper Scientific, PIXIS 100B-UV, SP-2150i). During the measurements, the sample position was controlled using a piezo motor stage (THK Precision) whose moving resolution is 20 nm in order to evaluate the photo-emission characteristics of a single micro-spherical particle. The morphologies of the micro-spherical particles were evaluated using a scanning electron microscope (SEM, HITACHI, SU8020).

3. Results and discussion

Figure 1(a) shows the typical photo-emission spectra of ZnO nanopowder assembly and a hierarchical micro-spherical particle prepared for 9 h and subsequently annealed at 400°C at pulsed pumping light irradiation. The inset shows the SEM images of the corresponding samples. Both samples show much narrower emission peaks with the width of below ~1 nm at a threshold pumping laser fluence than those of spontaneous band-edge PL emission for the nanopowder (~14 nm) [54] and for the micro-particle (~26 nm) shown in the figure S1 in Supplementary material. The sharp peaks for nanopowder assembly can be attributed to lasing oscillation due to random multiple light scattering of nanoparticles consisting of assembly[37]. In case of the hierarchical microparticle, it can be understood from the figure that the number of lasing peak mode for the micro-spherical particle is much smaller than that of the nanopowder assembly. The number of lasing modes for micro-spherical particle is confirmed to vary from sample-to-sample and the pumping fluence. The laser emissions with similar features are reported in the aggregate micro-spherical particle [47]. In addition, the spontaneous emission background PL emission seen in nanopowder assembly is considerably suppressed in the micro-spherical particle. Similar suppression of the spontaneous emission is observed in SiO_2 capped ZnO nanorod array with a rod

dimeter of ~100 nm [55]. These features indicate that optical confinement occurs in the case of the micro-spherical particle lasing oscillation. It should be noted that the discrete mode lasing from the different type of hierarchical microparticle, i.e., the urchin-like ZnO nanostructures, is reported in literature [50]. The possible origin of such a laser emission is discussed below in detail.

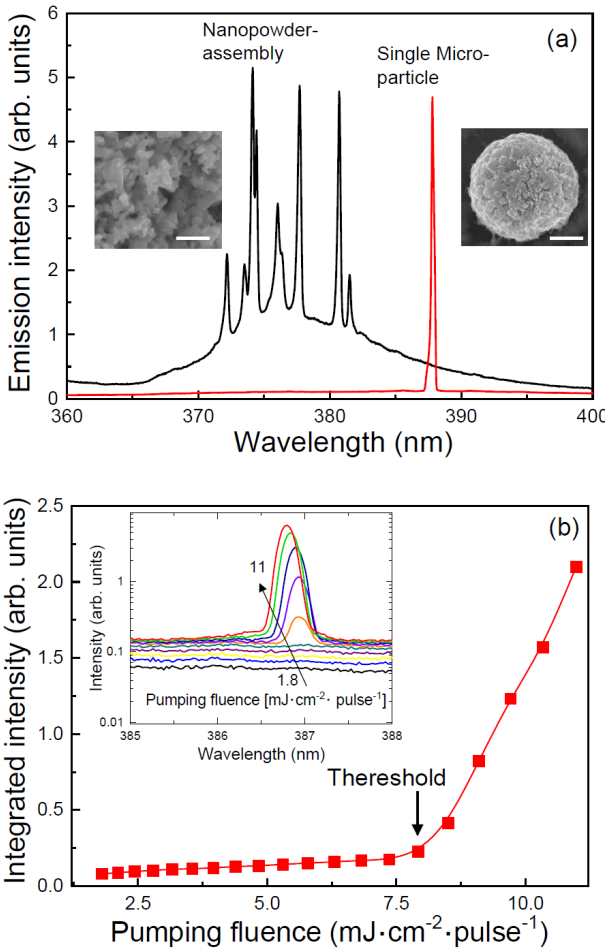

Figure 1. (a) Lasing emission spectra of a ZnO nanopowder-assembly and a single ZnO hierarchical micro-spherical particle sample. Insets show the SEM images of corresponding samples. The scale bar of the inset is 1 μm. (b) Integrated intensity of photo-emission from single ZnO hierarchical micro-spherical particle samples as a function of pumping laser fluence. Inset shows the photo-emission spectra for various pumping laser fluence.

Figure 1(b) shows the integrated photo-emission intensity as a function of the pumping laser fluence of the ZnO micro-spherical particle annealed at 400°C. The inset shows the corresponding spectra. From the figure, a typical threshold behavior is observed, i.e., the emission intensity nonlinearly increases at the threshold pumping fluence of 7.6 $\mathrm{mJ \cdot cm^{-2} \cdot pulse^{-1}}$. From the inset, it is confirmed that the lasing peak abruptly appears on the weak spontaneous PL emission background at the threshold. This threshold behavior is the clear evidence that lasing oscillation occurs in the presently prepared micro-spherical particle.

The blue shift of lasing peak with increasing pumping energy is observed as shown in the inset of figure 1(b). To clarify this behavior, the energy shift of lasing peak, ΔE_{l}, with respect to the lasing peak at the threshold (~7.91 $\mathrm{mJ/cm^2 \cdot pulse}$) is plotted in figure 2(a). The maximum value of ΔE_{l} shift is ~1.1 meV in the present pumping region. The similar blue shift increasing the pumping energy is reported in a single ZnO nanorod.[56] In that report, the blue shift is attributed to a refractive index change due to high density excitation of carriers and resultant formation of electron-hole plasma (EHP). Another possibility for the peak shift is that changes in the gain spectrum due to high carrier excitation through the lasing frequency pulling effect [57]. To clarify the underlying mechanism for the lasing peak shift, we calculated the excited carrier density dependence of gain spectra and refractive indexes based on a many-body theory [58]. We used essentially the same calculation parameters as our previous work [54] and the excited carrier density is estimated from the pumping fluence from the relation, $n = F/(E_{\mathrm{p}}D)$,[59,60] where F, E_{p} and D are pumping fluence, photon energy of pumping light (~3.49 eV), and the crystallite size (~30 nm), by assuming that an electron-hole pair is generated by an incident photon and all absorbed photons generate electron-hole pairs. Although the calculated values through the above relation may be overestimated because of neglecting the recombination lifetime of carriers, we can

safely understand that the excited carrier linearly depends on the pumping fluence. Note that spontaneous emission peak redshift and broadening with increasing the pumping fluence, i.e., the increase in the excited carriers, due to electron-hole plasma formation, which is typically observed in ZnO [59]. The estimated n is shown in upper horizontal axis of figure 2(a). The calculated refractive index dispersion and gain spectra are shown in the inset of figure 2(a) and figure S1 of the Supporting Information, respectively. As shown in the figure, the refractive index at the lasing energy (~3.20 eV) decreases due to the high carrier excitation effect. On the other hand, the gain peak shifts to higher energy side and its width increases with increasing the excited carrier density, arising from the band filling effect[58].

From the calculated data, we obtained the energy shift of lasing peak by simply assuming the frequency pulling effect,[57] $\Delta E_{\mathrm{l}} = \left(w_{\mathrm{c}}\Delta E_{\mathrm{ga}} + w_{\mathrm{ga}}\Delta E_{\mathrm{c}}\right)/\left(w_{\mathrm{c}} + w_{\mathrm{ga}}\right)$, where w_{c} and w_{ga} are cavity and gain damping parameters, and ΔE_{c}, and ΔE_{ga} represent the energy shift of gain peak and cavity resonance energy, respectively. The values of w_{ga} and E_{ga} were estimated from the gain spectral width and peak energy shown in figure S1. The value of w_{c} is fixed to be 1.8 meV estimated from the experimental lasing peak width. We consider that ΔE_{c} depends on the refractive index n of the gain material, and it can be calculated from the relation,[61] $\Delta E_{\mathrm{c}}/E_{\mathrm{c}} = S\Delta n/n$ where E_{c}, Δn and S are the resonance energy of the cavity, refractive index change of gain material, and the sensitivity of cavity resonance energy to n, which has been used for whispering galley mode micro-spherical particle laser. In figure 2(a), we plotted the calculated ΔE_{l} as a function of the excitation fluence as a solid curve. For a comparison purpose, we also plotted the calculated energy shift under the constant refractive index as the dashed curve in figure 2(a). The calculated results with considering the refractive index changes safely correspond to the experimental data, and the calculation with only the gain shift effect does not agree with the experimental data except

in a lower pumping fluence region. This strongly supports the conjecture that the energy shift of lasing peak is mainly due to high carrier excitation induced refractive index change.

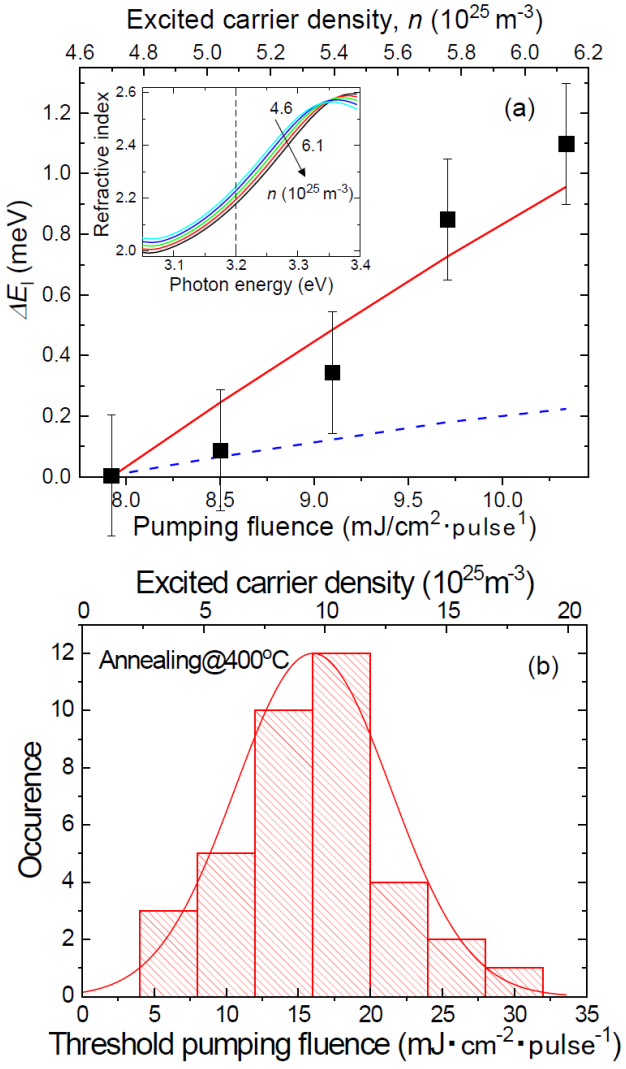

Figure 2. (a) Lasing peak shift ΔE_l as a function of the pumping fluence for the ZnO hierarchical micro-spherical particle. The solid and dashed curves represent the calculated ΔE_l with and without taking the excited carrier dependent refractive index changes into consideration, respectively. Inset shows excited carrier density dependent refractive index dispersion calculated by many-body theory.[54,58] (b) Lasing threshold histogram of pumping laser fluence for the

annealed ZnO hierarchical micro-spherical particle samples. Upper and lower horizontal axes are threshold excited carrier density and pumping fluence.

To further investigate the lasing characteristics of the hierarchical micro-spherical particle, we measured lasing thresholds for various micro-spherical particles and constructed the histogram as shown in figure 2(b). The threshold values are varied from 4 to 30 $\mathrm{mJ \cdot cm^{-2} \cdot pulse^{-1}}$, and the average and standard deviation of the threshold fluence are 15 and 5.7 $\mathrm{mJ \cdot cm^{-2} \cdot pulse^{-1}}$, respectively. We also estimated the threshold excited carrier densities to attain lasing by using the above-mentioned relation. The results are shown in the upper horizontal axis of figure 2(b). By comparing the theoretical calculated gain spectra shown in figure S1, sufficient optical gain is attained even at the lowest threshold carrier density, $\sim 2.4 \times 10^{25}$ $\mathrm{m^{-3}}$. Furthermore, the threshold densities are clearly larger than the Mott density ($\sim 1.8 \times 10^{24}$ $\mathrm{m^{-3}}$). indicating that the origin of the lasing emission from the present micro-spherical particle is EHP recombination, as similar to other types of random lasers.[54]

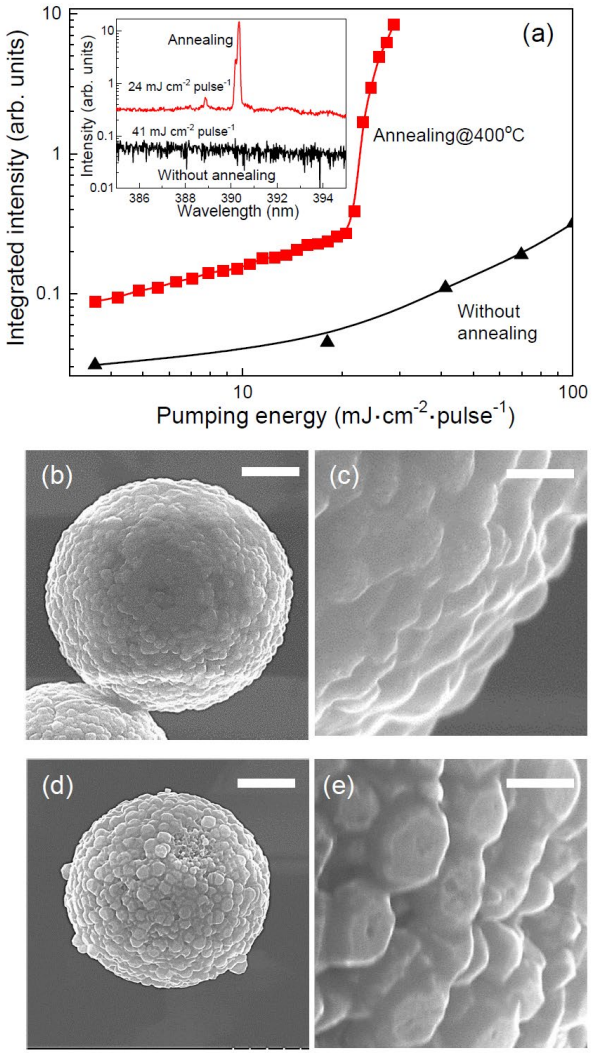

Figure 3. (a) Integrated intensity of photo-emission from as-prepared and annealed single ZnO hierarchical micro-spherical particle samples as a function of pumping laser light fluence. Inset shows corresponding emission spectra of the corresponding samples. SEM images of (b), (c) as-prepared and (d), (e) annealed ZnO hierarchical micro-spherical particle samples for different magnifications. The scale bar of (b) and (d) is 1 μm, and that of (c) and (e) is 200 nm.

Figure 3 and its inset shows the pumping fluence dependence of the emission intensity and typical emission spectra for as-prepared and annealed hierarchical micro-spherical particles at

400ºC. From these data, the lasing threshold behavior and lasing peak cannot be observed for the as-prepared sample in our pumping fluence region. One reason for this is insufficient net optical gain for lasing due to poor crystalline quality for the sample without annealing. In fact, as shown in figure S1 in the Supplementary Material, PL (spontaneous) emission intensity increases by annealing treatment due to the improvement of the crystallinity of ZnO [62]. The effects of crystalline quality on random lasing characteristics have been reported in literature [38,63]. To further examine the effect of annealing on scattering properties of the micro-spherical particle, the SEM images of the as-prepared and annealed samples are shown in figure 3(b)-3(e). It can be confirmed that the surface convexity increases by annealing from the comparison of the expanded SEM images between figure 3(c) and 3(e), indicating that the sizes of the nanoparticles consisting in the micro-spherical particle become larger by annealing. The larger sizes of the nanoparticle may induce the enhancement of light scattering, resulting in assisting the optical feedback for lasing. The role of size dependent scattering properties for the nanoparticles will be discussed in detail below.

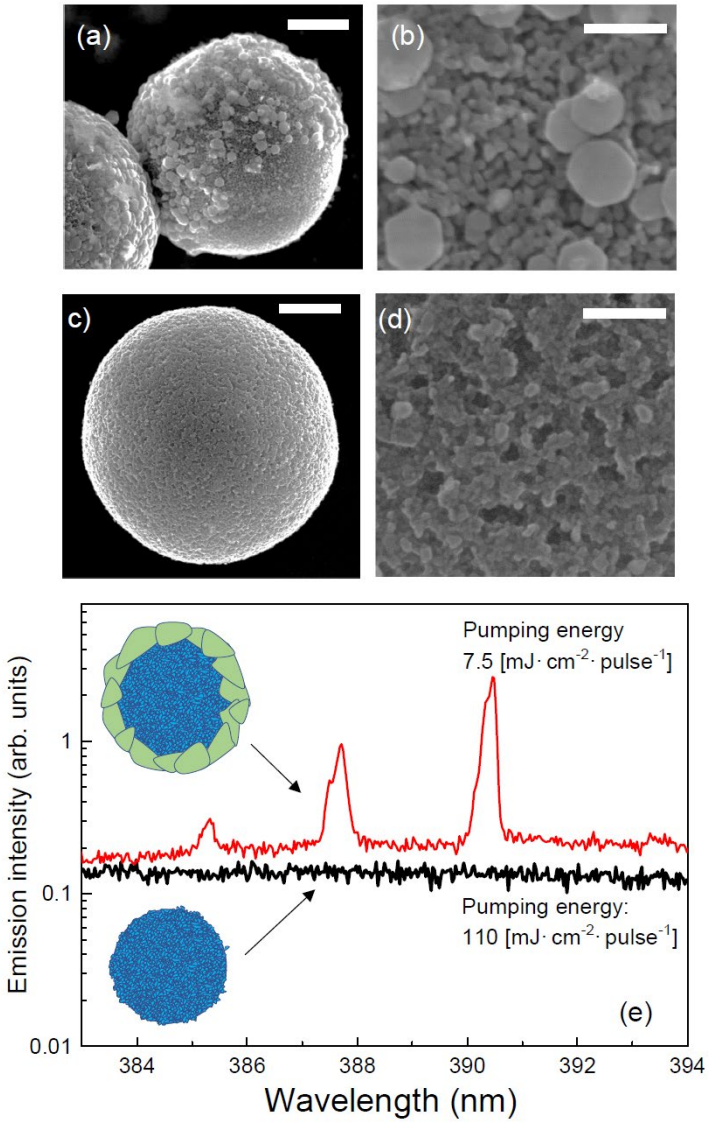

Figure 4. SEM images of (a), (b) a laser ablated ZnO hierarchical micro-spherical particle for solvothermal process for 9 h by irradiation of intense pumping laser light, and (c), (d) a ZnO hierarchical micro-spherical particle without outer larger plate-like nanoparticle prepared for solvothermal process for 12 h. The scale bar of (a) and (c) is 1 μm, and that of (b) and (d) is 200 nm. (e) Lasing emission spectra of a ZnO micro-spherical particle with and without larger plate-like nanoparticles. Insets show the schematic illustrations of the microparticle structures.

The light scattering efficiency is known to strongly depend on the size of scatterers. The micro-spherical particle prepared by solvothermal process for 9 h has a hierarchical structure consisting of outer large plate-like nanoparticles with a dimeter of tens of nanometers as shown in figure 3(c) and inner small nanoparticles with a diameter of several hundred nanometers.[52] Figure 4(a) and 4(b) show the SEM images of micro-spherical particle samples damaged at a high laser fluence irradiation. The surface plate-like nanoparticles are partly peeled off due to laser ablation effect and the inner nanostructures are appeared. The sizes of the inner nanoparticles are around 10~50 nm which is smaller than those of plate-like nanoparticles of 100~200 nm. To roughly examine the light scattering properties of these nanoparticles, we calculated the scattering efficiency Q_s of a single ZnO spherical particle based on Lorentz-Mie theory.[64] In the calculation, the refractive index dispersion of ZnO used is the values reported in the literature.[65] The calculation results are shown in figure S2(a) and S2(b) in the Supporting Information. At around lasing wavelength (~387 nm), the Q_s steeply increases for the sphere with the diameter of 100 nm, and it is peaked for 160 nm. Furthermore, as shown in the figure S2(b), the Q_s of the sphere with the diameter of 160 nm which corresponds to a typical outer plate-like nanoparticle size in the hierarchical micro-spherical particle exhibits a resonance peak at lasing wavelength region (385–395 nm). In addition, its values are much larger than that of the sphere with 30 nm in diameter corresponding to an inner nanoparticle size.

From the calculation results, we consider that the present hierarchical micro-spherical particle has two clear contrasting nanoparticle components as a point of view of light scattering, i.e., larger outer plate-like nanoparticles which are strong scatterers and smaller inner nanoparticle assembly which is regarded as a transparent layer for emitting light because of its weak scattering efficiency because of much smaller size than the emitted light wavelength. Thus, we can expect that lasing oscillation arises from the light scattering of outer plate-like nanoparticles. To confirm this

conjecture, we prepared a micro-spherical particle consisting of only ZnO nanoparticles with the diameter of several tens of nanometers by solvothermal process for 12 h as shown in the SEM images of figure 4(c) and 4(d) and evaluated the photo-emission properties at a higher pumping fluence. The typical photo-emission spectrum of the sample is presented in figure 4(e). We cannot observe the lasing emission from the micro-spherical particle without outer larger nanoparticles, despite sufficient light pumping. Therefore, we can understand that lasing oscillation of the hierarchical micro-spherical particle is due to the strong light scattering at the interface between inner smaller nanoparticle layer and outer larger nanoparticle layer, and resultant optical confinement in the micro-spherical particle. On the other hand, the nanoparticles of a few tens of nanometers in diameter do not provide sufficient light scattering to occur light confinement and the positive feedback, and the light emission of gain material (ZnO) is dissipated to the outside of the micro-spherical particle, resulting in high loss.

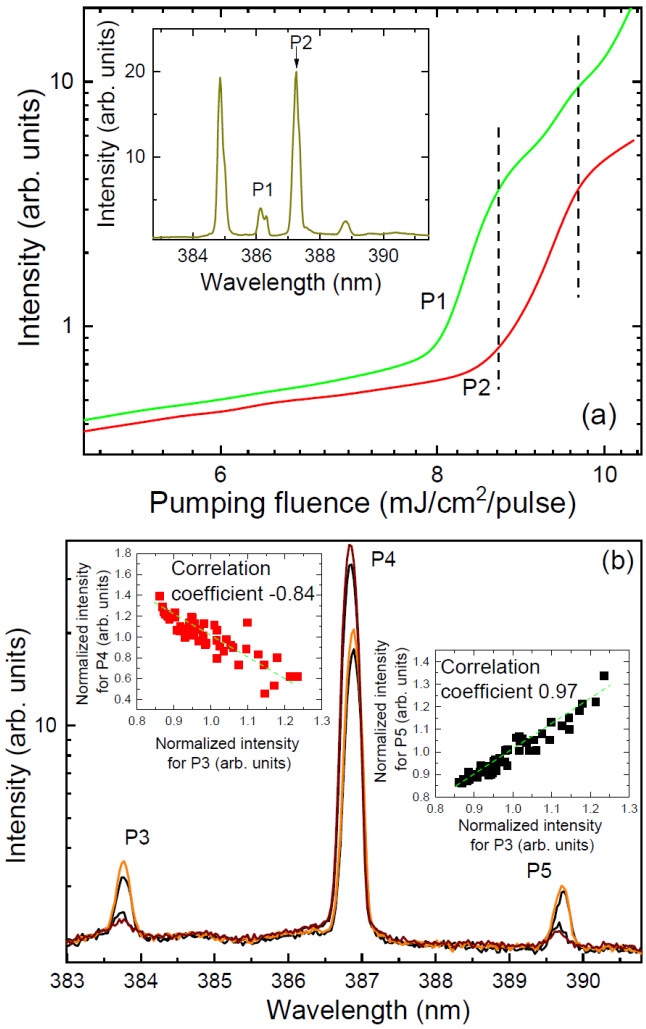

Figure 5. (a) Emission intensity vs. pumping fluence curves for the lasing peaks at 386.1 (P1) and 3787.2 nm (P2). Inset shows the corresponding spectra. (b) Shot-to-shot lasing emission spectra for a fixed pumping fluence. Insets show the correlations of the normalized lasing intensity between the peak at 383.7 (P3) and 386.8 nm (P4), and between 383.7 (P3) and 389.7 nm (P5), respectively.

The contribution of the outer nanoparticle scattering mentioned above possibly indicates that lasing oscillation is attributed to random multiple scattering feedback, i.e., random lasing. However, the present hierarchical micro-spherical particles show discrete mode lasing peaks

similar to the ordinary microcavity laser such as whispering galley mode (WGM) lasers [66], where the lasing oscillation occurs due to internal total refection at the boundary with definitely distinct modes. Then, to further clarify the lasing origin in the present system, we investigate the characteristics of each laser mode peaks of the hierarchical microparticle. Figure 5(a) and its inset show the pumping fluence versus emission intensity curves for different lasing peaks and the corresponding emission spectrum. From the inset, the spectral spacing between each lasing mode (vertical arrows) is irregular, i.e., the mode spacing is varied from 0.2~1.5 nm, while in the case of WGM laser, the lasing mode spacing is a nearly constant [67]. This irregular frequency mode feature is typically observed in the random laser, where the mode spacing is reported to be statistically fluctuated [68]. Furthermore, two kinks (vertical dashed lines) in the curves at 8.3 and 9.0 mJ/cm^2/pulse for the laser modes at 387.5 (P1) and 387.7 nm (P2) are clearly seen as shown in figure 5. This indicates that the lasing peak modes P1 and P2 compete with each other for acquiring limited optical gain in the ZnO micro-particle because of spatial overlap between the modes. Such a gain competition is also observed in the random laser system [68]. Moreover, we confirmed that the synchronized changes in the lasing peak intensity randomly occurs in the present micro-particle laser. Figure 5(b) shows various lasing spectra at a fixed laser fluence. As shown in the figure, the peak intensity at 386.9 nm (P4) changes with synchronizing those of the lasing peaks at 383.8 (P3) or 389.7 nm (P5). Insets of figure 5(b) show the correlations of normalized intensity between the peaks. The sign of correlation coefficient between P3 and P4 is negative (-0.84), indicating that the opposite intensity changes occur between them. On the other hand, the sign of that between P3 and P5 is positive (0.97), probably resulting from usual intensity fluctuations due to pumping fluence. These results suggest that the modes P3 (or P5) and P4 randomly exchange the optical energy with each other, indicating that the optical paths of the cavity modes for the feedback randomly changes. Such a mode interaction is typically reported in the random laser system [69].

Therefore, the origin of the lasing oscillation is random scattering feedback as well as the microcavity induced optical confinement, since the present microparticle has hybrid features between usual microcavity lasers and random lasers. Further analysis based on theoretical approaches such as a finite difference time domain method may be needed to clarify detailed lasing feedback mechanism in the present system.

4. Conclusion

In conclusion, we investigated the lasing characteristics of a hierarchical micro-spherical particle with diameters of 1 – 5 μm and discussed its lasing feedback mechanisms. The discrete sharp lasing emissions were observed for the micro-spherical particle. Theoretical calculations based on a many-body theory revealed that the clear optical gain is reached at the observed lowest lasing threshold value, $4\ \mathrm{mJ \cdot cm^{-2} \cdot pulse^{-1}}$, corresponding to the excited carrier density $\sim 2.4 \times 10^{25}\ \mathrm{m^{-3}}$. The threshold carrier density is higher than the reported Mott density, indicating that the lasing origin is EHP recombination. Furthermore, the lasing frequency mode shift (~1.2 meV) is due to the refractive index changes induced by increasing carrier density up to $6.1 \times 10^{25}\ \mathrm{m^{-3}}$. By performing theoretical calculations of the size dependent scattering efficiency of a ZnO sphere based on Mie theory, it is found that the efficiency is optimum at the diameter of ~160 nm , which falls into the size range of outer nanoparticles (100~200 nm) consisting in the hierarchal micro-sphere. These results suggest that the strong light scattering and resultant light confinement inside the micro-spherical particle contributing to the lasing oscillation occur at the interface between inner transparent layer consisting of small nanoparticles (10-60 nm) and the outer strong light scattered nanoparticle layer consisting of the hierarchical micro-spherical particle. We also observed the strong lasing mode interaction effects. The features of the present microparticle system indicate random lasing oscillation accompanying microcavity confinement effect occurs.

To further control the size distribution of the nanoparticles and hierarchy of the structure, we could tune the resonance frequency of random cavities and attain a lower lasing threshold. The present findings would be beneficial for optimization of the micro-spherical particle based random laser for future concise and low-cost micro-laser devices.

ASSOCIATED CONTENT

Supplementary material

PL spectra of hierarchical micro-sphere particle, and calculation results of gain spectra from a many-body theory and scattering efficiency of a spherical ZnO particle from Lorenz-Mie theory.

AUTHOR INFORMATION

Corresponding Authors *E-mail: nakamura@hosei.ac.jp

Notes

The authors declare no competing financial interest.

ACKNOWLEDGMENT

The authors would like to thank Prof. Fujiwara (Hokkai Gakuen University) for useful discussion.

REFERENCES

[1] Hayashi I, Panish M B, Foy. P W and Sumski S 1970 Junction lasers which operate continuously at room temperature *Appl Phys Lett* **17** 109

[2] Alferov Zh I, Andreev V M, Garbuzov D Z, Zhilyaev Yu V., Morozov E P, Portnoi E L and Trofim V G 1970 Effect of heterostructure parameters on the laser threshold current and the realization of continuous generation at room temperature *Soviet Physics Semiconductors* **4** 1573

[3] Kressel H and Hawrylo F Z 1970 Fabry-Perot structure AlxGa1−xAs injection lasers with room-temperature threshold current densities of 2530 A/cm2 *Appl Phys Lett* **17** 169

[4] Casey H C and Panish M B 1978 Optical Fields and Wave Propagation *Heterostructure Lasers* ed H C Casey and M B Panish (New York: Academic Press) p 20

[5] Lawandy N M, Balachandran R, Gomes A and Sauvain E 1994 Laser action in strongly scattering media *Nature* **368** 436–438

[6] Wiersma D S 2008 The physics and applications of random lasers *Nat Phys* **4** 359–367

[7] Andreasen J, Sebbah P and Vanneste C 2011 Coherent instabilities in random lasers *Phys Rev A (Coll Park)* **84** 023826

[8] Nakamura T, Takahashi T and Adachi S 2010 Temperature dependence of GaAs random laser characteristics *Physical Reiview B* **81** 125324

[9] Redding B, Choma M a. and Cao H 2012 Speckle-free laser imaging using random laser illumination *Nat Photonics* **6** 355–9

[10] El-Dardiry R, Faez S and Lagendijk A 2011 Classification of light sources and their interaction with active and passive environments *Phys Rev A (Coll Park)* **83** 1–4

[11] Meng X, Fujita K, Murai S and Konishi J 2010 Random lasing in ballistic and diffusive regimes for macroporous silica-based systems with tunable scattering strength *Opt Express* **18** 1922–4

[12] Tulek A, Polson R C and Vardeny Z V. 2010 Naturally occurring resonators in random lasing of π-conjugated polymer films *Nat Phys* **6** 303–10

[13] Kitur J, Zhu G, Bahoura M and Noginov M a 2010 Dependence of the random laser behavior on the concentrations of dye and scatterers *Journal of Optics* **12** 024009

[14] Mai H H, Nguyen T T, Nguyen T T, To T T, Nguyen T T, Choi Y, Choi W and Ta V D 2022 Random lasers from the natural inverse photonic glass structure of Artemia eggshells *J Phys D Appl Phys* **55**

[15] Maryam W, Tan H H, Jagadish C, Dawes J M, Zhao B and Ismail W W 2022 A hybrid random laser using dye with self-organized GaN nanorods *Semicond Sci Technol* **37** 025009

[16] Janeczko M, Karpinski P, Mysliwiec J and Cyprych K 2023 Deep-blue random lasing emission coming from the BN-heteroacenes derivatives *Opt Mater (Amst)* **143** 114150

[17] Szukalska A, Zajac D, Cyprych K and Mysliwiec J 2023 Ultra-Photostable Random Lasing Coming from the Benzothiadiazole Derivative Dye-Doped Organic System *The Journal of Physical Chemistry C* **127** 24618–25

[18] Noginov M, Fowlkes I, Zhu G and Novak J 2004 Neodymium random lasers operating in different pumping regimes *J Mod Opt* **51** 2543–53

[19] Noginov M a, Novak J, Grigsby D and Deych L 2006 Applicability of the diffusion model to random lasers with non-resonant feedback *Journal of Optics A: Pure and Applied Optics* **8** S285–95

[20] Noginov M a., Zhu G, Frantz a. a., Novak J, Williams S N and Fowlkes I 2004 Dependence of NdSc 3 (BO 3) 4 random laser parameters on particle size *Journal of the Optical Society of America B* **21** 191

[21] Cao H, Zhao Y, Ong H and Ho S 1998 Ultraviolet lasing in resonators formed by scattering in semiconductor polycrystalline films *Appl Phys Lett* **73** 3656

[22] Noginov M a., Zhu G, Fowlkes I and Bahoura M 2004 GaAs random laser *Laser Phys Lett* **1** 291–3

[23] Fujiwara H and Sasaki K 2018 Amplified spontaneous emission from a surface-modified GaN film fabricated under pulsed intense UV laser irradiation *Appl Phys Lett* **113** 171606

[24] Shi Q, Fujiwara H, Kajita S, Yasuhara R, Tanaka H, Ohno N and Uehara H 2023 Structural Correlation of Random Lasing Performance in Plasma-Induced Surface-Modified Gallium Nitride *ACS Applied Optical Materials* **1** 412–20

[25] Chen Y, Herrnsdorf J, Guilhabert B, Zhang Y, Watson I M, Gu E, Laurand N and Dawson M D 2011 Colloidal quantum dot random laser *Opt Express* **19** 2996

[26] Dang C, Lee J, Breen C, Steckel J S, Coe-Sullivan S and Nurmikko A 2012 Red, green and blue lasing enabled by single-exciton gain in colloidal quantum dot films *Nat Nanotechnol* **7** 335–9

[27] Yakunin S, Protesescu L, Krieg F, Bodnarchuk M I, Nedelcu G, Humer M, De Luca G, Fiebig M, Heiss W and Kovalenko M V. 2015 Low-threshold amplified spontaneous emission and lasing from colloidal nanocrystals of caesium lead halide perovskites *Nat Commun* **6**

[28] Wang L, Yang M, Zhang S, Niu C and Lv Y 2022 Perovskite Random Lasers, Process and Prospects *Micromachines (Basel)* **13**

[29] Mamaeva M P, Samsonova A Y, Murzin A O, Lozhkina O A, Murashkina A A, Selivanov N I and Kapitonov Y V. 2022 Ultrafast Random Lasing in MAPbI3Halide Perovskite Single Crystals *Journal of Physical Chemistry C* **126** 19816–21

[30] Fruhling C, Wang K, Chowdhury S, Xu X, Simon J, Kildishev A, Dou L, Meng X, Boltasseva A and Shalaev V M 2023 Coherent Random Lasing in Subwavelength Quasi-2D Perovskites *Laser Photon Rev* **17**

[31] Zhan Z, Liu Z, Du J, Huang S, Li Q, Hu Z, Luo J, Yang Y, Dong S, Wang L, Tang J and Leng Y 2023 Thermally Evaporated MAPbBr3 Perovskite Random Laser with Improved Speckle-Free Laser Imaging *ACS Photonics* **10** 3077–86

[32] Chirvony V S, Suárez I, Sanchez-Diaz J, Sánchez R S, Rodríguez-Romero J, Mora-Seró I and Martínez-Pastor J P 2023 Unusual Spectrally Reproducible and High Q-Factor Random Lasing in Polycrystalline Tin Perovskite Films *Advanced Materials* **35**

[33] Wang J, Chen Q, Xu C, Cao Y, Song T, Li T, Xu X, Chen P and Xu L 2023 Low-threshold green and red random lasing emission in inorganic halide lead perovskite microcrystals with plasmonic and interferential enhancement *Ceram Int* **49** 9185–90

[34] Ma X, Chen P, Li D, Zhang Y and Yang D 2007 Electrically pumped ZnO film ultraviolet random lasers on silicon substrate *Appl Phys Lett* **91** 251109

[35] Consoli A, Caselli N and López C 2022 Electrically driven random lasing from a modified Fabry–Pérot laser diode-supplement- *Nat Photonics* **16** 219–25

[36] Consoli A, García P D and López C 2023 Tuning the emission properties of electrically pumped semiconductor random lasers via controlled pulsed laser ablation *Opt Express* **31** 42439

[37] Cao H, Zhao Y, Ho S, Seelig E, Wang Q and Chang R 1999 Random Laser Action in Semiconductor Powder *Phys Rev Lett* **82** 2278–81

[38] Fallert J, Dietz R, Hauser M, Stelzl F, Klingshirn C and Kalt H 2009 Random lasing in ZnO nanocrystals *J Lumin* **129** 1685–1688

[39] Umanskaya S F, Shevchenko M A, Tcherniega N V., Maresev A N, Matrokhin A A, Karpov M A and Voronova V V. 2023 Tuning the efficiency of Random Laser Generation in a Suspension of ZnO Nanoparticles by Means of its Directional Freezing *Journal of Russian Laser Research* **44** 691–9

[40] Huang M, Mao S, Feick H, Yan H and Wu Y 2001 Room-temperature ultraviolet nanowire nanolasers *Science (1979)* **1897**

[41] Azmi A N, Wan Ahmad Kamil W M, Abu Hassan H, Wan Ismail W Z and Muskens O L 2023 Random lasing behaviour in Al-doped ZnO nanorods *Opt Mater (Amst)* **138** 113718

[42] Azmi A N, Yong P S and Ahmad Kamil W M W 2022 Ex-situ doping of ZnO structures as potential random lasers *J Phys Conf Ser* **2411** 0–9

[43] Rashidi M, Haggren T, Jagadish C and Tan H H 2022 Characteristics and Thermal Control of Random and Fabry-Pérot Lasing in Nanowire Arrays *ACS Photonics* **9** 3573–83

[44] Rosli N, Halim M M, Kamil W M W A, Hashim M R, Hsu H C, Zhuang J Y and Siyuan C 2022 Random Lasing Emission of ZnO Nanorods from Different Seeding Thickness *J Phys Conf Ser* **2411**

[45] Bittner S, Knitter S, Liew S F and Cao H 2019 Random-laser dynamics with temporally modulated pump *Phys Rev A (Coll Park)* **99** 1–6

[46] Cao H, Xu J Y, Seelig E W and Chang R P H 2000 Microlaser made of disordered media *Appl Phys Lett* **76** 2997

[47] Cao H, Xu J, Zhang D and Chang S 2000 Spatial confinement of laser light in active random media *Phys Rev Lett* **84** 5548

[48] Nakamura T, Sonoda S, Yamamoto T and Adachi S 2015 Discrete-mode ZnO microparticle random laser *Opt Lett* **40** 2661–4

[49] Nakamura T, Yamamoto T and Adachi S 2015 Temperature dependence of lasing characteristics of irregular-shaped-microparticle ZnO laser *Opt Express* **23** 28905

[50] Lu C H, Chao T Y, Chiu Y F, Tseng S Y and Hsu H C 2014 Enhanced optical confinement and lasing characteristics of individual urchin-like ZnO microstructures prepared by oxidation of metallic Zn *Nanoscale Res Lett* **9**

[51] Matsumoto K, Saito N, Mitate T, Hojo J, Inada M and Haneda H 2009 Surface polarity determination of ZnO spherical particles synthesized via solvothermal route *Cryst Growth Des* **9** 5014–6

[52] Saito N, Matsumoto K, Watanabe K, Hashiguchi M, Sakaguchi I and Haneda H 2015 Microscopic and isotope tracer study on the growth of spherical ZnO particles in water-ethylene glycol solvent *Cryst Growth Des* **15** 2609–19

[53] Saito N and Haneda H 2011 Hierarchical structures of ZnO spherical particles synthesized solvothermally *Sci Technol Adv Mater* **12** 064707

[54] Nakamura T, Firdaus K and Adachi S 2012 Electron-hole plasma lasing in a ZnO random laser *Phys Rev B* **86** 205103

[55] Ali A T, Maryam W, Huang Y W, Hsu H C, Ahmed N M, Zainal N and Jameel M S 2022 SiO2 Capped-ZnO nanorods for enhanced random laser emission *Opt Laser Technol* **147**

[56] Fallert J, Stelzl F, Zhou H, Reiser A, Sauer R, Klingshirn C and Kalt H 2008 Lasing dynamics in single ZnO nanorods *Opt Express* **16** 919–23

[57] Siegman A E 1986 Fundamentals of Laser Oscillation *Lasers* (Califronia: University Science Books) p 457

[58] Versteegh M a. M, Kuis T, Stoof H T C and Dijkhuis J I 2011 Ultrafast screening and carrier dynamics in ZnO: Theory and experiment *Phys Rev B* **84** 1–19

[59] Klingshirn C, Hauschild R, Fallert J and Kalt H 2007 Room-temperature stimulated emission of ZnO: Alternatives to excitonic lasing *Phys Rev B* **75** 1–9

[60] Versteegh M, Vanmaekelbergh D and Dijkhuis J 2012 Room-Temperature Laser Emission of ZnO Nanowires Explained by Many-Body Theory *Phys Rev Lett* **108** 1–5

[61] Foreman M R, Swaim J D and Vollmer F 2015 Whispering gallery mode sensors: erratum *Adv Opt Photonics* **7** 632

[62] Saito N, Haneda H, Sekiguchi T, Ishigaki T and Koumoto K 2004 Effect of Postdeposition Annealing on Luminescence from Zinc Oxide Patterns Prepared by the Electroless Deposition Process *J Electrochem Soc* **151** H169

[63] Ali A T, Maryam W, Huang Y W, Hsu H C, Ahmed N M, Hassan H A and Zainal N 2022 Random lasing from gold-doped zinc oxide nanorods *Opt Mater (Amst)* **132** 112776

[64] Bohren C F and Huffman D R 1998 *Absorption and Scattering of Light by Small Particles* (Wiley)

[65] Adachi S 1997 Zinc Oxide (ZnO) *Optical Constants of Crystalline and Amorphous Semiconductors: Numerical Data and Graphical Information* pp 65–98

[66] Xu C, Dai J, Zhu G, Zhu G, Lin Y, Li J and Shi Z 2014 Whispering-gallery mode lasing in ZnO microcavities *Laser Photon Rev* **8** 469–94

[67] Yang S, Wang Y and Sun H D 2015 Advances and Prospects for Whispering Gallery Mode Microcavities *Adv Opt Mater* **3** 1136–62

[68] van der Molen K, Tjerkstra R, Mosk A and Lagendijk A 2007 Spatial Extent of Random Laser Modes *Phys Rev Lett* **98** 3–6

[69] Cao H, Jiang X, Ling Y, Xu J and Soukoulis C 2003 Mode repulsion and mode coupling in random lasers *Phys Rev B* **67** 1–4